Environ Geol (2006) 50: 505–524
DOI 10.1007/s00254-006-0228-y

ORIGINAL ARTICLE

F. Bozzano
S. Martino
M. Priori

Natural and man-induced stress evolution of slopes: the Monte Mario hill in Rome

Received: 28 December 2005
Accepted: 17 February 2006
Published online: 27 April 2006

Research activities were carried on with the co-operation of D'Arcangelo A. (Consorzio TREESSE, andrea.darcangelo@libero.it) and Moretti S. (IMG S.r.l. Servizi Tecnici per l'Ingegneria e l'Ambiente, moretti@img-srl.it)

F. Bozzano · S. Martino (✉)
Dipartimento di Scienze della Terra,
Università di Roma "La Sapienza",
P.le A.Moro 5, 00185 Rome, Italy
E-mail: salvatore.martino@uniroma1.it

M. Priori
Sezione Geologica, Eco Edilizia
Depurazioni, Rome, Italy
E-mail: m.priori@eco-edilizia.it

Abstract The paper deals with stress-release effects induced by man-made cuts or excavations into natural stiff clay slopes that experienced erosion in response to valley deepening. The study was focused on the Monte Mario hill in Rome (Italy), which formed part of an area of recent urban expansion. The methodology of the study relied on a reference engineering-geology model, which was developed on the basis of site and laboratory data and stress–strain analyses. The latter analyses were carried out with the finite-difference code FLAC 4.0. Numerical modelling was based on a sequential approach, taking into account the main evolutionary stages of the Tiber river valley in Rome's urban area and then making cuts at the bottom of the slope located south of the Monte Mario Astronomical Observatory. The simulation revealed the stress-release effects that fluvial erosion and excavation fronts have caused on the investigated slopes and their consequent gravitational instabilities. These processes appear with metre-scale displacements, followed by stress-release cracks (actually observed on the slopes under review). In quantifying stress-release deformations, the simulation took into account the possible role of creep in the observed retardation of stress-release effects.

Keywords Stiff clays · Stress-release · Man-made cuts · Slope stability · Numerical models

Introduction

Gravity-induced instabilities of stiff clay slopes have aroused the interest of engineering geologists for at least three decades (Calabresi and Scarpelli 1985; Calabresi 2004). Burland et al. (1977) reported the initiation of fractures in the walls of an excavation made into over-consolidated clays (Oxford clays). The authors emphasised their correlation with excavation works, but recognised that the phenomenon might depend on site conditions (seepage and initial stress) and on mechanical behaviour of the material (deformation moduli).

Retarded response of stiff clay slopes to stress-release processes (long-term stability) was attributed to various factors, such as dissipation of negative excess pore pressures (Chandler and Skempton 1974; Vaughan 1994; Potts et al. 1997; Dixon and Bromhead 2002; Amorosi et al. 2004) and creep (Tavenas and Leroueil 1980; Leroueil 2001). Cooper et al. (1998) described the results of an experimental cut made into the Gault Clays (England) and of real-scale monitoring. The study revealed progressive failure, which was retarded by dissipation of pore overpressure as a consequence of stress-release.

Macro- and micro-scale jointing and/or fissuring of stiff clays play a crucial role in the above-mentioned processes (Esu 1966; Skempton 1977): oriented discontinuities within stiff clays control their strength, deformability and behaviour at low levels of stress (Rampello and Silvestri 1993; Burland et al. 1999). In these cases the propagation of cracks according to a genetic model similar to the one proposed by Griffith (1920) justifies the observed brittle failure (Calabresi

et al.1990). In particular, Burland et al. (1999) pointed out that, at low levels of stress, the strength of stiff-fissured clays exceeds the available strength assessed from the intrinsic curve of the material. By contrast, at higher levels of stress, the opposite takes place. For the materials under review, also the representativeness of laboratory tests at specimen-scale is questioned (Calabresi et al. 1990; Calabresi 2004), having acknowledged the role of discontinuities within the rock mass and the influence of their orientation (Cancelli and Chinaglia 1993). An implicit limitation of triaxial tests on stiff-fissured clays is the representativeness of the peak strength that is measured on the specimen after appearance of a rupture surface (Calabresi et al. 1990).

In stress–strain analyses via numerical models (Potts 2003), the geotechnical complexity of stiff clays is not negligible. On the basis of the experience acquired over the past three decades, various simulation approaches have been developed to take into account the geomechanical properties of the investigated materials, their heterogeneity and the role of discontinuities observed on their outcrops. Duncan and Dunlop (1969) assessed the role of initial stress conditions (in terms of K_0) via finite-element modelling, noting that highly overconsolidated clays ($0.81 \leq K_0 \leq 1.60$) had a worse response to stress-release, owing to higher horizontal stresses. Potts (2003) addressed the issue of transferring complex engineering-geology models into computational codes for a more realistic numerical stress–strain analysis. The author presented a summary of applications from an extensive international case history. Previously, Vaughan (1994) had proposed the use of parameters from both laboratory and site tests for a more realistic numerical simulation of clayey slope stability. Vaughan identified delayed deformation effects on stiff clay slopes, ascribing them to the dissipation of excess pore pressures and initial confinement conditions. Constitutive laws taking into account the decay in the strength of the material were used to reconstruct the distribution of strength values, highlighting progressive failure along the rupture surface (Leroueil 2001). Calabresi et al. (1990) recognised the need to fine-tune the numerical simulation of the geomechanical behaviour of stiff-fissured clays by using softening laws at different levels of stress. More recently, Hicks and Samy (2002) took into account the heterogeneity of stiff clays by associating them with statistically varying parameters with normal or Gaussian distributions and by introducing spatial control functions (Griffith and Fenton 2000).

Matheson and Thomson (1973) investigated the role of the unloading induced by natural processes, such as fluvial erosion, and underlined the role of stress rebound in the decay of the deformability characteristics of the affected rocks. Stress release due to natural processes is compounded by topography- and gravity-induced distortions of the stress field (McTingue and Mei 1981; Savage et al. 1985), as compared to the more regular lithostatic distribution, which is in turn governed by the regional stress field (Haneberg 1999). In some instances, these distortions may be sufficient to produce instability or failure (Miller and Dunne 1996). Man-made changes in topography, such as cuts and excavations, may cause additional distortions of the stress field, which can be expressed in terms of K variations (Duncan and Dunlop 1969; Matheson and Thomson 1973).

The here reported case study investigated the instabilities which were detected in the stiff-fissured clays (''Marne Vaticane'' *Auct.*) of the Monte Mario hill, in Rome's urban area (Fig. 1). These instabilities depend on a combination of stress-release factors: fluvial erosion, which led to the present configuration of the Tiber river valley, and vertical man-made cuts at the foot of the slopes. The cuts were made extensively in historical times (Fig. 2), initially for clay quarrying and then for new settlements in an area of strong urban expansion (Figs. 3, 4).

Stiff-fissured clays with geotechnical properties similar to the ''Marne Vaticane'' widely outcrop all over Italy. The methodology adopted in this study can thus be applied to similar engineering-geology contexts.

The approach adopted in the study involved the numerical simulation of stresses and strains in the investigated slopes and the reconstruction of the main erosional stages of the Tiber River valley (in Rome's urban area) and of subsequent man-induced effects. On the basis of both laboratory tests and site observations, the numerical simulation took into account the variability of geomechanical parameters with confinement, thus accommodating the complexity of the geological model of the investigated slopes.

Geological setting of the Tiber river valley in the area of Rome

About 35% of Rome's historical centre presently rests on the alluvia of the Tiber river and of its tributaries (Fig. 5). The basin of the Tiber (with a drainage area of about 17,000 km^2) consists of carbonate, volcanic and siliciclastic rocks.

Rome's present urban area experienced marine sedimentation until the lower Pleistocene (Fig. 5). The Monte Mario, Vaticano and Gianicolo hills, located on the right bank of the Tiber, hold records of a pelitic succession of lower-upper Pliocene age: the ''Marne Vaticane'' unit. This unit has a discordant contact with the upper Monte Mario unit: a lower Pleistocene succession composed of silty sands. The upper part of this succession represents the top of the Monte Mario hill [144 m above sea level (a.s.l.)], i.e. Rome's topographically highest relief.

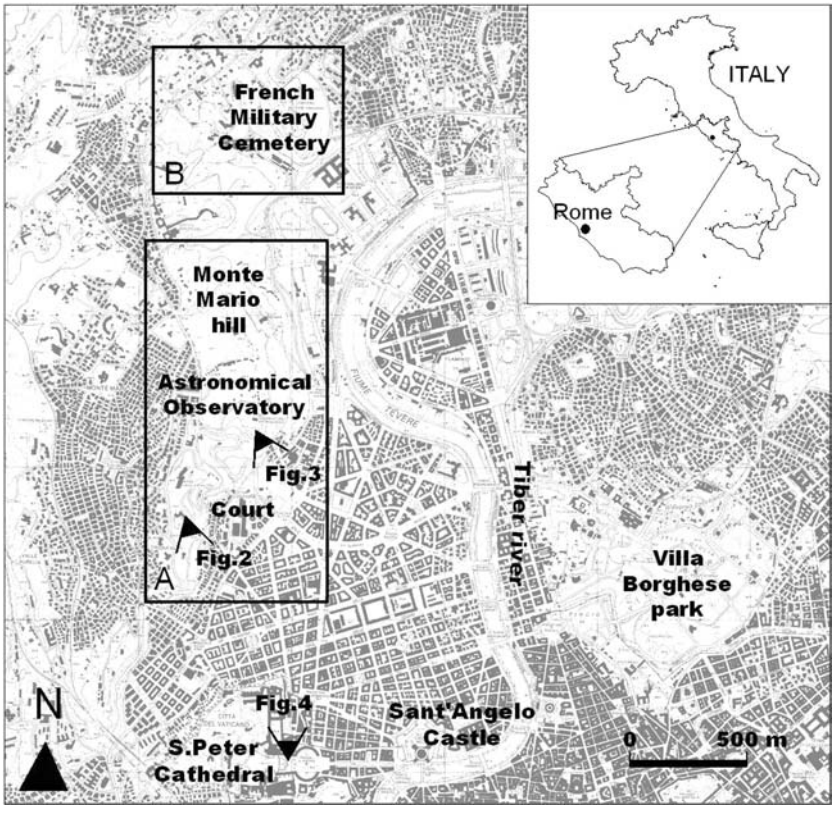

Fig. 1 Location of the Monte Mario hill in Rome's urban area; the *boxes* refer to the geological sketches of Fig. 7; the photo-points of view are referred to Figs. 2, 3 and 4

Fig. 2 View of the "Valle dell'Inferno" valley in the 1910s from Monte Mario hill (see Fig. 1): to be noticed are the chimneys of the clay kilns and the scarps of the quarries of "Marne Vaticane" stiff clays

Subsequently, from the middle Pleistocene to Present, the geological evolution of the area occurred in a marine-to-continental transition environment, culminating into the development of the Tiber river deltaic and alluvial system and of the nearby coastal plain (Fig. 6). In this time interval, the sequence of erosional and depositional events resulted from the combination of the following processes:

- Glacioeustatic sea level fluctuations, from 22 to 1 MIS (Marine Oxygen Isotope Stage);
- Tectonic pulses of relative uplift and/or lowering, which affected various sectors of this peri-Tyrrhenian area;
- Volcanic activity of the Sabatino and Alban Districts, starting from about 800 and 600 ky (i.e. 600,000 years), respectively.

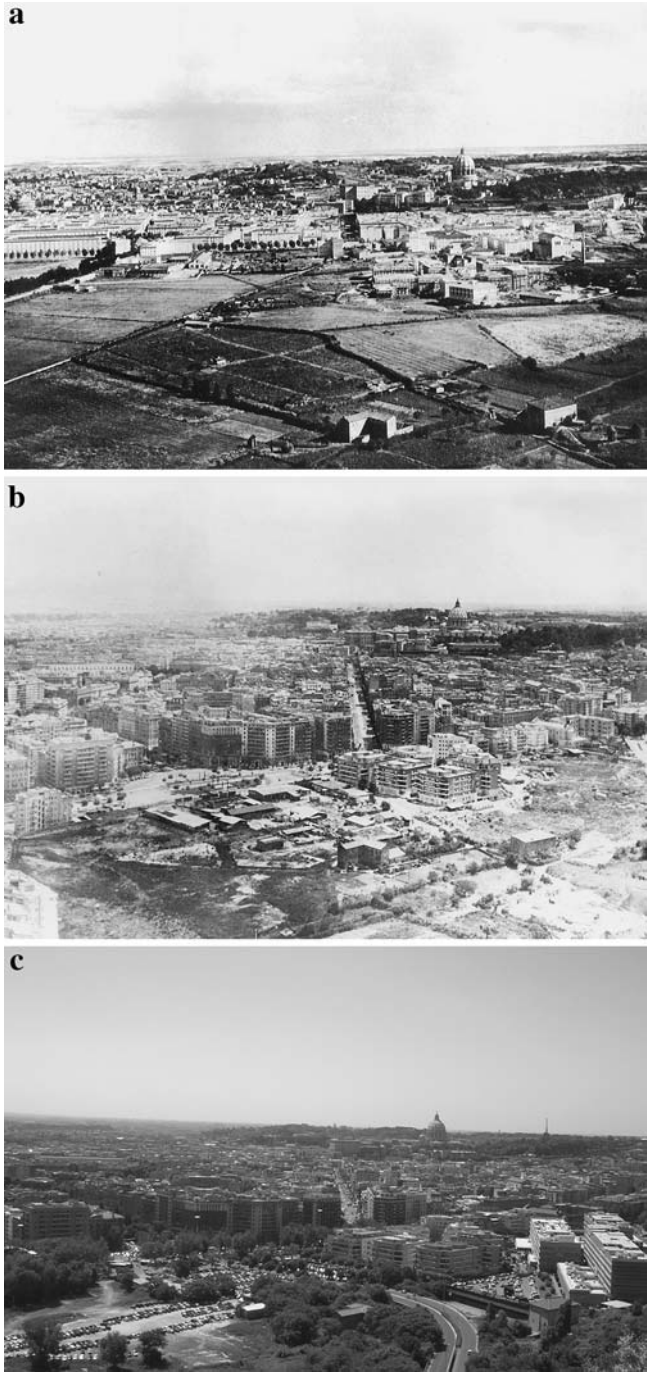

Fig. 3 Comparison of the Prati district in the 1910s (**a**), in the 1960s (**b**) and in the 1990s (**c**) from the Astronomical Observatory of the Monte Mario hill (see Fig. 1) to highlight the urban expansion

Recently, various authors (Milli 1997; Karner and Marra 1998; Karner et al. 2001a, b; Giordano et al. 2003) explained the complex sedimentary record deriving from the interaction of the above-listed processes as a temporal sequence of different depositional units (sequences or synthemes). Both the sedimentary deposits and their contacts were identified and correlated in Rome's urban sector. A complex series of pre-volcanic and syn-volcanic sedimentary units were distinguished. The first of the syn-volcanic units (Santa Cecilia unit) has an estimated age of about 600 ky; the last one, of Holocene age, was deposited during the Flandrian transgression (13 ky-Present) during a volcanically quiescent period.

In Rome's urban area, after the development of the "Monte Ciocci" unit (MIS 22-21 transition) (Fig. 6a) and until Present, this evolution is testified by: alternating episodes of erosional deepening of the hydrographic network, in periods of sea level low-stand; subsequent partial or total filling of valley furrows, in some cases associated with tectonic dislocations (e.g. PalaeoTiber graben), in periods of sea level high-stand.

Close to the Monte Mario hill, on the left bank of the Tiber river, is the most ancient erosion surface. This surface was recognised in the "Marne Vaticane" unit and can be observed at an elevation of about 20–25 m a.s.l. at the foot of the Pincio hill (De Angelis D'Ossat 1942). In the literature, the sedimentary cover of this surface is ascribed to the pre-volcanic depositional unit of the PalaeoTiber 1 (Marra and Rosa 1995a) (Fig. 6b). Hence, this surface might mark the maximum depth of erosion reached about 780 ky BP at MIS 20 (Karner et al. 2001a, b). Conversely, the most recent erosion surface is carved into the "Marne Vaticane" stiff clays, which represent the bedrock, at an elevation of about 45 m b.s.l. This surface, lying beneath the present alluvial plain of the Tiber river, shows the maximum level of valley incision that the river reached during the glacial low-stand of sea level corresponding to the Wurm glaciation, about 18 ky BP (Fig. 6c). The subsequent filling of the Tiber valley during the last glacial termination (13 ky) created the recent alluvial deposit of the Tiber river, whose maximum thickness is about 60 m (Bozzano et al. 2000) (Fig. 6d).

Today, these alluvia represent sedimentary deposits with fairly complex geometries. Therefore, for the sake of simplicity, these deposits are grouped here into three lithotypes, overlain by fill material (Bozzano et al. 2000):

(a) Polygenic gravels with centimetre-scale clasts embedded in a sandy–silty matrix; average thickness 8 m; lithotype G;
(b) Alternating grey silty clays, clayey silts and sandy silts with interbedded peat levels; overall average thickness 30 m; lithotypes C and D;
(c) Silty sands with pebbles and sandy silts of dark brown to grey colour, evolving upwards into silts and clayey silts; average thickness 15 m; lithotypes A and B.

Fig. 4 Comparison of the foot hill of Monte Mario in the 1910s (**a**) and in 1990s (**b**) from St. Peter's Dome (see Fig. 1) to highlight the urban expansion

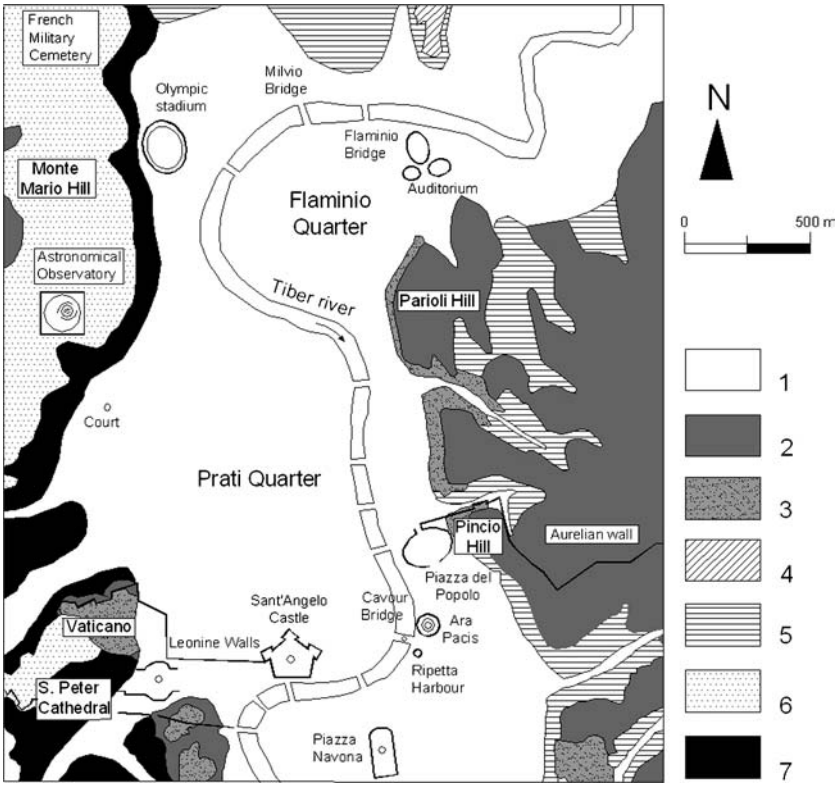

Fig. 5 Geological sketch of Rome's northern area (modified from Bozzano et al. 2000): *1* Tiber river recent alluvia and man-made fills (Holocene to Present); *2* Volcanic unit (middle to upper Pleistocene); *3* syn-volcanic unit (middle to upper Pleistocene); *4* fluvio-lacustrine PalaeoTiber unit (middle Pleistocene); *5* PalaeoTiber unit (middle Pleistocene); *6* Monte Mario unit (lower Pleistocene); *7* "Marne Vaticane" unit (middle to upper Pliocene)

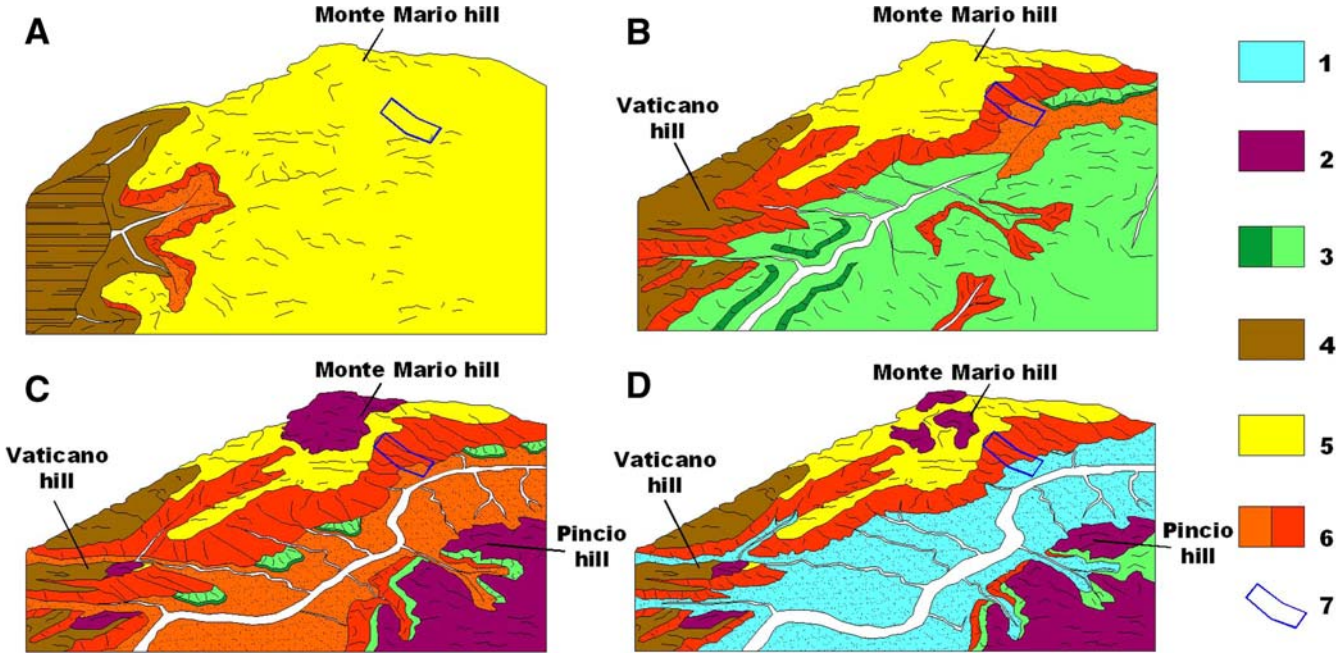

Fig. 6 Three-dimensional sketches of the main evolutionary stages of Rome's northern area: **a** deposition of the "Monte Ciocci" formation (about 900 ky); **b** partial deepening of the Tiber valley (about 800 ky); **c** further deepening of the Tiber valley during the Wurmian glacial low-stand (18 ky); **d** Holocene Tiber alluviation during the Flandrian transgression (13 ky). *1* Holocene alluvia, *2* Volcanic unit, *3* Ponte Galeria formation, *4* "Monte Ciocci" formation, *5* Monte Mario unit, *6* "Marne Vaticane" unit, *7* area including the section of Fig. 12

Geological-stratigraphic setting of the Monte Mario hill

The most ancient deposits outcropping on the Monte Mario hill (Fig. 7) are ascribed to the "Marne Vaticane" unit ("Monte Vaticano", *Auct.*). This unit, representing the bedrock of the entire Roman area, consists of marine deposits from an outer circalittoral environment. These well-bedded deposits are made up of silty clays interbedded with silty sands; the thickness of the layers ranges from few centimetres to some decimetres. Their clayey strata are of grey colour with conchoid fracture; they display scarce carbonaceous frustules and no macrofossils. The interlayered beige or yellow sands are very dense and rarely weakly cemented. The measured dip of the "Marne Vaticane" strata, in the entire Monte Mario hill area, is from subhorizontal to about 20°.

The age of these sediments is widely debated in the specific literature (Carboni 1975; Marra and Rosa 1995a; Bergamin et al. 2000; Cosentino et al. 2004): from lower Pliocene to upper Pliocene and also to lower Pleistocene.

During excavations for construction of the "Passante a Nord Ovest" tunnel (northern portion of the Monte Mario hill), this lithotype demonstrated to have experienced tectonic displacements prior to deposition of the Monte Mario unit (Fig. 8). These movements generated NW-SE-trending and NE- and SW-dipping fault planes, with throws of up to some tens of metres (A. D'Arcangelo, 2003, unpublished data).

The "Marne Vaticane" clays (violet in Fig. 8) are unconformably overlain by sandy–silty terms (yellow in Fig. 8) referable to the Monte Mario unit and of presumable lower Pleistocene age (Ambrosetti and Bonadonna 1967; Belluomini 1985; Malatesta and Zarlenga 1986; Marra et al. 1998; Marra 1993; Cosentino et al. 2004).

The transgression dividing the Monte Mario unit from the Monte Vaticano one (reported by Bonadonna 1968, and confirmed by surveys on the "Passante a Nord Ovest" tunnel excavation front) places the "Marne Vaticane" clays in contact with the "Limi di Farneto" silts. In the Monte Mario area, outcrops of these silts have an average thickness of 15 m. The "Limi di Farneto" (Marra and Rosa 1995a, b) formation consists of alternating clayey silts of grey colour with whitish concretions and organic remnants and fine-grained sandy levels of brown colour ("Unità di Monte Mario", Marra and Rosa 1995a, b; Lower Pleistocene. "Formazione di Ponte Galeria", Bellotti et al. 1994; Middle Pleistocene). On the top of the "Limi di Farneto" a 2 m thick level of grey sands with "Artica Islandica" is present ("Sabbie grigie ad Artica Islandica", Conato et al. 1980; Cosentino et al. 2004). Over the "Sabbie grigie ad Artica Islandica" are the Sabbie Gialle sands of the Monte Mario unit (Bonadonna 1968; Conato et al. 1980), whose average thickness in the Monte Mario area exceeds 50 m. These are medium-fine silty quartz sands

with occasional macrofossils, generally cohesionless. Discontinuous levels of sandstone, up to 50 cm thick, as well as levels up to 3.5 m thick, composed of highly cemented bioclastic rock (''Panchina a Brachiopodi'') are also observed; these levels outcrop at an elevation of 80–115 m a.s.l. and their lateral continuity is limited to about 100 m.

Upwards, the Monte Mario unit (Bellotti et al. 1994; Marra and Rosa 1995a, b) terminates into a alternating yellowish sand and grey-greenish lagoonal clay deposit with highly decalcified shell remains; this deposit, known as ''Argille verdi a Cerastoderma Lamarckii'', has a maximum thickness of 2–3 m (Bonadonna 1968).

Also the Monte Mario deposits have evidence of tectonic discontinuities (Section II of Fig. 7). In particular, in the northern sector of the Monte Mario hill, these deposits are dislocated by NW-SE- and NNE-SSW-trending normal faults with throws of up to 40 m. These discontinuities are supposed to originate from Pleistocene tectonic displacements, which presumably gave rise to the Monte Mario horst, reported to be 700–600 ky old by Giordano et al. (2003). In some places, the Monte Mario deposits have a 260/8 dip direction/dip, whereas they are subhorizontal in the area south of the Astronomical Observatory. The contact between the ''Marne Vaticane'' unit and the Monte Mario unit lies at

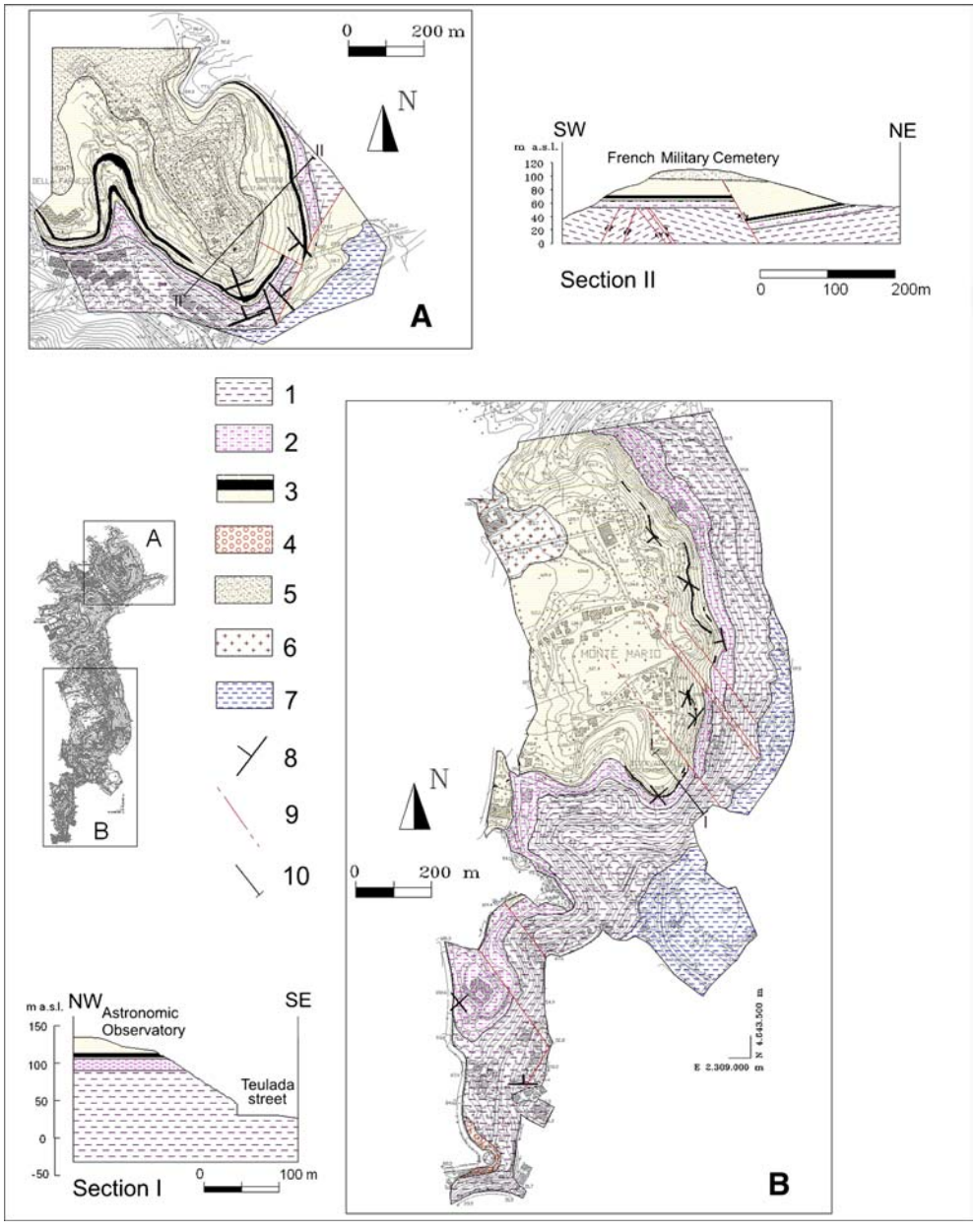

Fig. 7 Geological map, geological sections of the investigated areas. *1* Silty clays of grey-blue colour, with interbedded decimetre-scale levels of havana-brown fine-grained sands (''Marne Vaticane'' unit; lower Pliocene-lower Pleistocene); *2* Clayey silts of grey colour and fine-grained sandy levels of brown colour (''Limi di Farneto'' formation; lower Pleistocene); *3* Medium/fine-grained sands of yellow colour with highly cemented bioclastic rock (''Panchina a Brachiopodi'' levels; lower Pleistocene-middle Pleistocene); *4* Loose sands of yellow colour, medium- to coarse-grained, interbedded with decimetre-scale levels and lenticular bodies of gravels (''Monte Ciocci'' unit; middle Pleistocene); *5* Coarse-grained sand and silt of red-brown colour (middle Pleistocene); *6* Brown-yellowish stratified tuffs and fluvio-lacustrine deposits (middle-upper Pleistocene); *7* Alluvial deposit (Holocene). *8* Attitude of beds; *9* Fault; *10* Trace of geological section

elevations ranging from 50 m under the Collina dei Francesi hill to 65 m a.s.l. in the area north of the Astronomical Observatory and to about 95 m a.s.l. more southwards. This setting is probably due to the occurrence of faults that affect the entire sedimentary succession.

North of the Monte Mario hill (French Military Cemetery), the Monte Mario unit is unconformably overlain by red-brown medium-coarse sands and silts, without sedimentary structures and frequent centimetre-scale ferrous inclusions (''Sabbie eoliche rubefatte'', Bonadonna 1968; ''Formazione di Ponte Galeria'', Bellotti et al. 1994).

Deposits ascribable to the ''Monte Ciocci'' unit outcrop in the southernmost portion of the Monte Mario hill. These deposits are made up of yellow loose sands of medium-coarse grain size, with centimetre-scale levels and lenses of calcareous-siliceous gravel whose clasts have a maximum diameter of 1 cm. Their overall thickness in the entire Monte Mario area does not exceed 5 m. On the southern side of the Monte Mario hill, man-made cuts have records of the transgressive contact

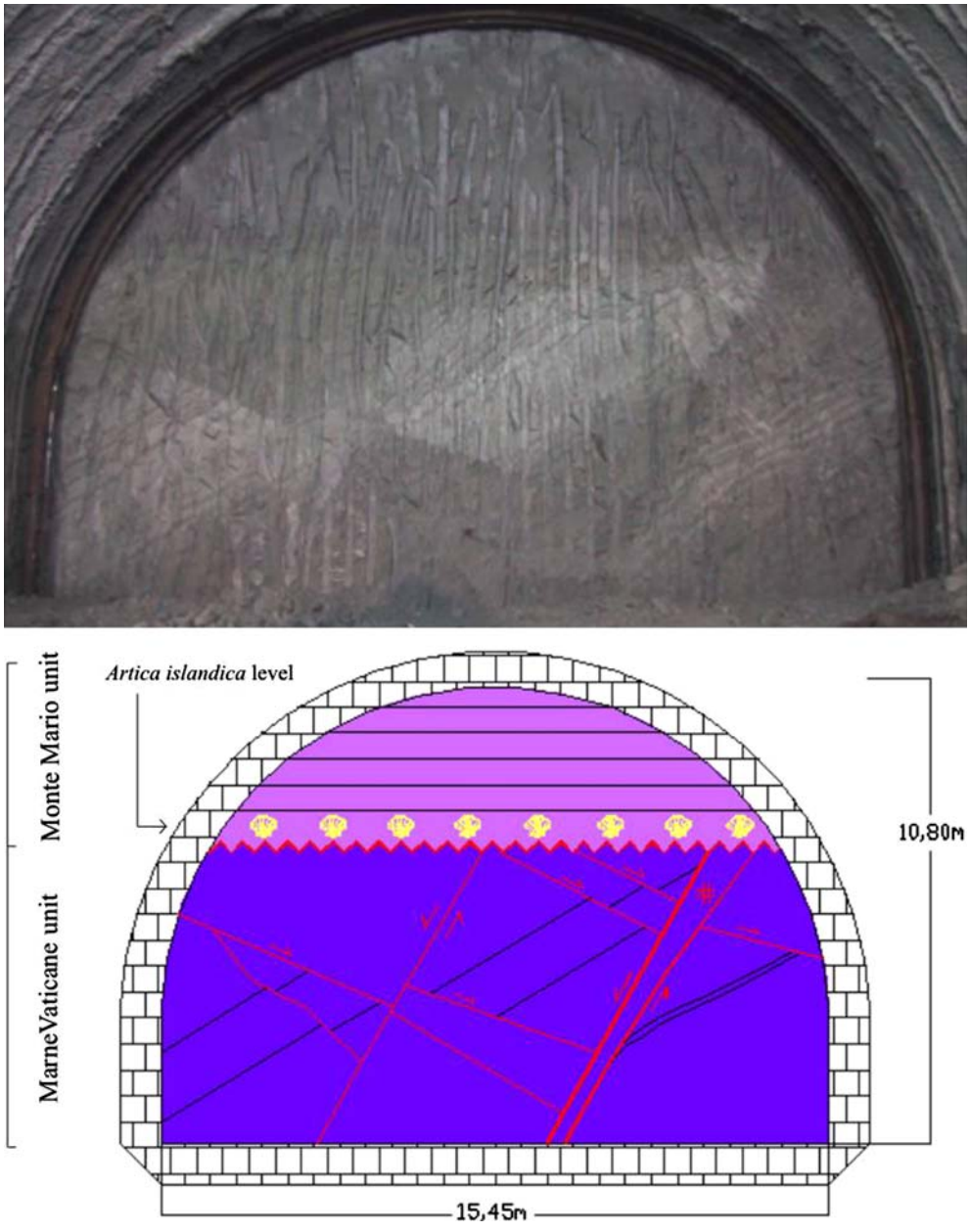

Fig. 8 Excavation front of the ''Passante a NW di Monte Mario'' tunnel: note the transgression of the Monte Mario unit over the ''Marne Vaticane'' unit and the tectonisation of the ''Marne Vaticane'' unit (*red lines*)

of the "Monte Ciocci" unit over the "Monte Vaticano" one.

Volcanic deposits from the Sabatino District are only exposed in the north-western sector of the Monte Mario hilltop. These deposits, which are likely to be part of the "Tufi Stratificati Varicolori di Sacrofano" unit (Ventriglia 2002), have a presumable age of about 450 ky (Karner et al. 2001a). They primarily consist of stratified tuffs of brown-yellowish colour, with frequent grey pumiceous levels of grey colour. In some places, fluvio-lacustrine deposits of volcanoclastic materials (epiclastites) are encountered (part of "Tufi antichi", Ventriglia 2002).

East of the Monte Mario hill, the bottom of the slopes has an alluvial cover, deposited after the last glacial termination and having a thickness of up to 60 m (Bozzano et al. 2000). They are composed of clayey and clayey–sandy deposits; at the base a gravel layer of some metres thick is present. Above lies variably thick fill material, accumulated after the foundation of Rome (700 years BC).

Gravitational processes on the Monte Mario hill

The Monte Mario hill is subject to diffuse landsliding. Shallow movements, which may topple tall trees and remove some cubic metres of soil trapped in the roots, are dominant. Falls are concentrated in areas of exposure of "Panchina a Brachiopodi" levels, from which blocks of up to some cubic metres may be dislodged. These blocks may roll along the slope at a distance of some tens of metres. The slopes consisting of the "Limi di Farneto" silts and of the "Sabbie di Monte Mario" sands and with no exposure of "Panchina a Brachiopodi" are subject to roto-traslational slides. These slides produced sandy–silty superficial debris somewhere involved in small flow-like movement.

Tension cracks were also observed within the "Marne Vaticane" unit, on the slope east of the Astronomical Observatory. The slope was undercut in the 1950s to accommodate a few buildings.

The first report of a crack leads back to June 1998 when some leakage from the fire hydrants was signalled (Fig. 9c). This crack was almost completely obliterated by weathering and erosion processes.

From July to October 2002, various cracks appeared in the same sector of the slope (Fig. 9a, b); these cracks were mapped at a scale of 1:200 (Fig. 9c).

Most of the cracks have a main curvilinear alignment and downslope concavities. Along the alignment, the cracks have a maximum throw of 1.1 m. Minor cracks tends to close further downslope. The chord linking the ends of the main crack has a length of 50 m. A scarp with decreasing height towards NE gives evidence of this crack.

The appearance of the above-described cracks on the slope east of the Monte Mario Observatory is likely to be closely dependent on bottom-slope man-made cuts, as substantiated by technical documentation and reports of anthropogenic actions on the slope.

Indeed, beginning in the 1920s, progressive urbanisation involved the search for new settlement areas on the Monte Mario hill slopes. To accommodate buildings, use was made of abandoned quarry sites and, subsequently, cuts were made at the bottom of the slopes. The study is focused on one of these slopes.

The frequency of man-made cuts into the "Marne Vaticane" clays is justified by their composition, which has made them suitable as building material since Roman times. From this period on, the clays have been used first to make adobe bricks and then, with the construction of numerous brick kilns throughout the area, for making brick clay building components (Spina 1958; Gigli 1971). What remains of these brick kilns, which were present in many Roman suburbs until some decades ago, are a number of place names ("Valle dell'Inferno", "Monti di Creta"). Especially in the northern sector of Rome, the opening of huge bench-shaped quarries (IGM 1924; Marino and Gigli 1934) made it necessary to level wide areas, which were subsequently occupied by urban districts (Fig. 2). Many of these quarry faces are still visible in the southernmost sector of the Monte Mario hill (Via Labriola and Piazzale Socrate).

In particular, the slope located east of the Monte Mario Observatory experienced various urbanisation stages, which were reconstructed as follows (summary in Table 1):

1. In a map of 1906, the slope appears as the steepest one of the entire hill (map of Istituto Cartografico Italiano, in Frutaz 1962).
2. In the map of Rome, published by Marino and Mauro Gigli in 1934 (Frutaz 1962), no cuts are discernible on the slope.
3. In 1955, a subvertical scarp, sharply breaking the slope, was visible (map of Direzione Generale del Catasto, in Frutaz 1962).
4. In 1959, as shown by aerial photographs (E.T.A. Society, in Frutaz 1962), some buildings and a retaining wall were constructed.
5. During the period elapsing from the construction of the wall and the 1980s, struts were placed between the retaining wall and the buildings in order to support the wall (Ventriglia 1986).
6. In 1986, a technical report indicated apparently shallow instabilities uphill of the retaining wall (Ventriglia 1986).

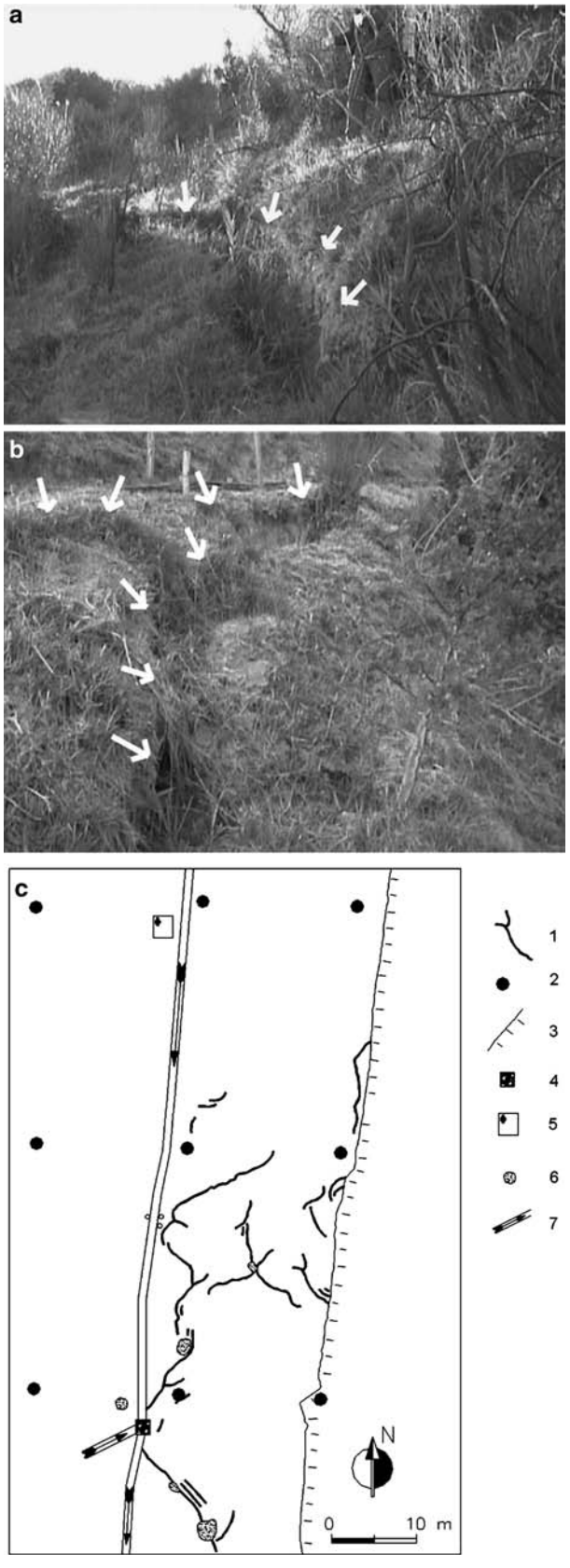

Fig. 9 **a**, **b** Cracks in the slope south of the Astronomical Observatory marked with *white arrows* pointing downslope; **c** map of the survey made on 21st November 2002: *1* cracks; *2* benchmarks installed in 1998; *3* scarps; *4* rainwater collection pits; *5* fire hydrants; *6* shrub vegetation; *7* runoff drainage channels

7. Therefore in 1986, wall consolidation works were proposed in order to reduce the lateral stresses due to the struts, which caused damages to the building anchored to the retaining wall (Ventriglia 1986).
8. In June 1998, the first fracture was reported on the slope at an approximate elevation of 70 m a.s.l. and at a distance of about 50 m from the wall.
9. From July to October 2002, after a summer with intense precipitation, numerous cracks appeared in the same area.
10. In September 2003, some fractures occurred further west of the above cracks, at an elevation of 80–90 m a.s.l. and at a distance of about 70 m from the wall.

Geotechnical laboratory characterisation of the "Marne Vaticane" unit

Given the diffuse landsliding of the "Marne Vaticane" outcrops in the Monte Mario area, geotechnical laboratory tests were conducted to characterise their mechanical behaviour at low confining pressures. Use was made of undisturbed block-samples, which were taken from the excavation fronts of the "Passante a NW" tunnel. The physical properties and Atterberg limits of the "Marne Vaticane" clays are summarised in Table 2.

The mechanical behaviour of the stiff clays ascribable to the "Marne Vaticane" unit was analysed via CID and CIU triaxial tests. Specimen preparation took into account the orientation of primary anisotropies (bedding), due to the silty–sandy intercalations that are typical of the "Marne Vaticane" unit, versus the direction of the imposed maximum principal stress. However, the behaviour of the investigated lithology was analysed in more detail by considering the primary anisotropies both orthogonal and parallel to the imposed maximum principal stress. The selected confining pressure range represents site conditions down to a depth of 50 m b.g.l.; in particular, a 10–700 kPa confining pressure range was selected for primary anisotropies orthogonal to the maximum principal stress, while a 200–700 kPa was selected for primary anisotropies parallel to the maximum principal stress. A wider confining pressure range was adopted for primary anisotropies orthogonal to the maximum principal stress, as this condition corresponds to the in-site attitude of the "Marne Vaticane" clays.

Table 1 Historical events on the Monte Mario slope starting in the nineteenth century

Year	Source	Type of document	Event
1839	Congregazione del Censo	Map	Presence of a villa at the foot of the slope (Villa Franchetti)
1900	Genio Militare	Map	Presence of a scarp NW of Villa
1906	Istituto Cartografica italiano	Map	Very steep slope
1934	A. Marino and M. Gigli	Map	Absence of man-made cuts uphill of Villa Franchetti
1955	Direzione Generate del Catasto	Map	Presence of a subvertical scarp at the foot of the slope
1959	Società E.T.A.	Aerial Photos	Construction of a few buildings and of a retaining wall
1970–1980(?)	U. Ventriglia	Technical report	Placing of struts between the retaining wall and the buildings' downslope
1986	U. Ventriglia	Technical report	Appearance of shallow instabilities uphill of the retaining wall; damages to the buildings
1985–1990(?)	U. Ventriglia	Technical report	Increase in the number of drainage holes in the wall; insertion of bars to anchor the wall to the slope; removal of struts
1998	A. Prestininzi and F. Bozzano	Technical report for Municipality of Rome—X Department	Appearance of a crack at an elevation of 70 m a.s.l., about 50 m away from the wall
2002	M. Priori	Degree thesis sponsored by Roma Natura Agency	Numerous cracks appeared in the same zone from July to October
2003	M. Priori	Degree thesis sponsored by Roma Natura Agency	Appearance of a crack uphill of previous ones (at an elevation of 80–90 m a.s.l.) in September

Stress–strain properties at low stress levels were tested in detail, considering the number of man-induced actions on slopes where the "Marne Vaticane" stiff clays outcrop (opening of quarries, excavations or road cuts) and the consequent changes induced in their stress–strain conditions.

During the triaxial tests, the material proved to have a dilating behaviour and the measured dilatance angle was about 14°.

Specimens with anisotropies orthogonal to the maximum principal stress showed a 24° friction angle and a 25.5 kPa cohesion, whilst specimens with anisotropies parallel to the maximum principal stress showed a 25° friction angle and a 175 kPa cohesion (Fig. 10a; Table 2).

At low levels of stress (only for anisotropies orthogonal to the maximum principal stress), the shear strength significantly drops, as the confining pressure decreases from 100 to 10 kPa. Also the measured stiffness significantly decreases in the same range of confining pressure; in particular, the elastic modulus (E_t) falls from 80.9 to 17.2 MPa, whereas the elasto-plastic secant modulus (E_s) declines from 44.9 to 11.8 MPa (Fig. 11).

Moreover, undrained strength parameter values ($\varphi_{cu} = 25°$ and $c_u = 200$ kPa) were obtained from CIU triaxial tests.

Table 2 Physical and mechanical properties of "Marne Vaticane" silty-clays from laboratory triaxial and oedometer tests

	Horizontally oriented anisotropies		Vertically oriented anisotropies
γ_n (kN/m^3)		20.6	
γ_d (kN/m^3)		17.0	
γ_s (kN/m^3)		26.5	
W_n (%)		21	
S_n (%)		100	
e_0		0.55	
n		0.35	
W_{LL} (%)		46	
W_{LP} (%)		18	
Pl (%)		28	
Sand (%)		14	
Silt (%)		50	
Clay (%)		36	
OCR	6.7		5.6
σ_y (Pa)	6.15E + 06		5.15E + 06
C_R	0.06		0.06
C_c	0.29		0.31
C_s	0.07		0.09
φ_{cu} (°)		25	
c_u (Pa)		2.00E + 05	
φ (°)	24		25
c (Pa)	2.55E + 04		1.75E + 05
ψ (°)	14		14

All the parameter values obtained from triaxial tests are summarised in Table 2, together with the compressibility parameters obtained from oedometer tests by considering primary anisotropies both orthogonal and parallel to the vertical stress.

On the basis of all the results from laboratory tests, best fitting functions (Asef and Reddish 2002) were obtained representing the variation of both shear strength parameters (shear strength angle and cohesion intercept) (Fig. 10b, c) and stiffness (E_t and E_s moduli) (Fig. 11) with confining pressure. Since the latter is in turn indicative of depth, the resulting functions evidenced a significant decrease in both shear strength and stiffness at very low confining pressures (< 50 kPa), corresponding to a depth of roughly 10 m b.g.l. This behaviour, which may also be predicted from Griffith's envelope, may be attributed to the high OCR (6.7) of the investigated stiff clays (Calabresi et al. 1990; Rampello and Silvestri 1993; Burland et al. 1999).

Numerical stress–strain analysis

The collected geological, geomorphological and engineering-geology data made it possible to model the gravitational instability processes affecting the Monte Mario hill slopes, as a consequence of their incision by the Tiber river and by recent man-made cuts.

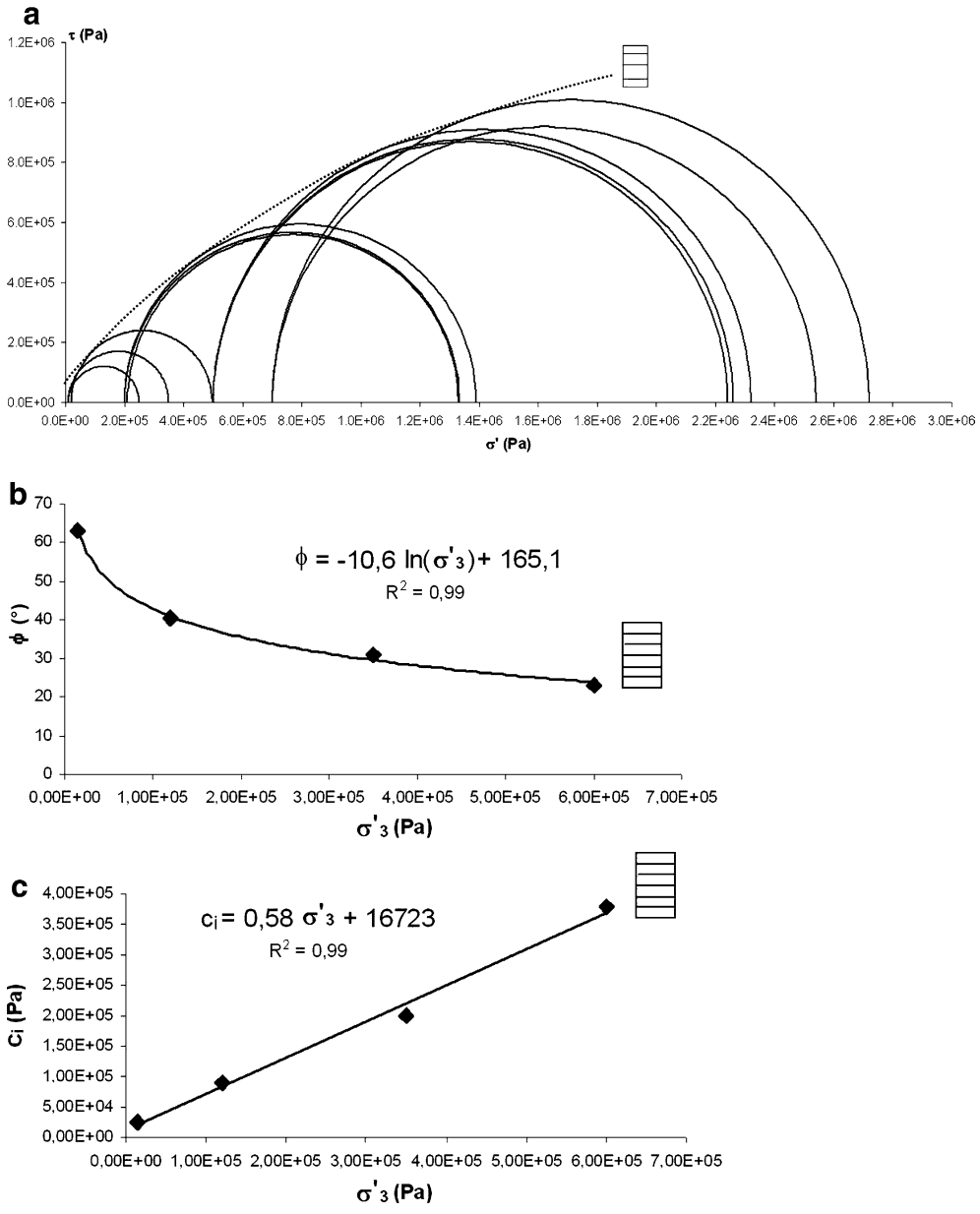

Fig. 10 **a** Mohr envelope obtained from triaxial tests on "Marne Vaticane" specimens with anisotropies oriented normally to σ'_1; **b** φ versus σ'_3 experimental function; **c** c (intercept) versus σ'_3 experimental function

On this basis, it may be assumed that both natural and man-induced stress-release are responsible for the observed instability processes.

To validate this assumption, a stress–strain analysis was conducted in order to model the stress-release induced both by the emplacement of the Tiber valley (until its present morphological configuration) and by man-made cuts at the bottom of its nearby slopes.

The analysis was carried out along two geological sections, for which the respective engineering-geology models were defined (Fig. 12): the first section (A) was obtained transversally to the present Tiber valley for a length of about 1,500 m, starting from the Monte Mario hilltop near the Astronomical Observatory; the second one (B) was laid over the previous one for a length of 550 m, starting from the Monte Mario hilltop.

The two engineering-geology sections were simulated via the finite-difference code FLAC 4.0 (Itasca 2000), by using square-mesh grids with a resolution of 10 m for section A and of 2.5 m for section B. The selected code responded to the requirement of using an explicit temporal solution to better simulate the stress–strain behaviour of continuous media up to large deformations.

For the stress–strain analysis of the investigated slopes, a sequential simulation approach was adopted, by modelling the assumed evolutionary conditions on the same section and using output data from the previous step as input data for the next step of the sequence.

Numerical simulations conformed to the Mohr–Coulomb elastic-perfectly plastic constitutive law; the values assigned to the parameters (Table 3) were taken from the literature, except for the "Marne Vaticane" lithotype, which was characterised during the laboratory tests described above.

As plotted in Fig. 12, the steps of the simulation were as follows:

1. Section A (step 1): deposition of Plio-Pleistocene sediments in a succession supposed to be continuous with planar morphology;
2. Section A (step 2): excavation of the first palaeovalley by the Tiber river, after deposition of Pleistocene marine sediments, in a period of time ranging from 870 to 530 ky. The valley palaeomorphology was assumed to be similar to the present one, i.e. a "basin" configuration with an average slope angle of 22°. Valley deepening (110 m) was quantified as the difference in height between the Monte Mario hilltop (144 m a.s.l.) and the bottom of the deposits referable to the PalaeoTiber 1 (Marra and Rosa 1995a, b) and exposed in the Pincio-Trinità dei Monti area at approximately 20 m a.s.l.
3. Section A (step 3): further deepening of the Tiber valley, beginning at about 18 ky, to a depth of about −45 m b.s.l. (Bozzano et al. 2000), with an overall difference in height of 190 m with respect to the Monte Mario hilltop.
4. Section A (step 4): Deposition of alluvia (present throughout Rome's historical centre) up to 20–25 m a.s.l. (Bozzano et al. 2000), starting from about 13 ky.
5. Section B (step 5): transfer of the stress–strain solutions obtained in step 4 from section A to section B (with higher resolution).
6. Section B (step 6): simulation (under undrained conditions) of man-made cut at the bottom of the slope east of the Astronomical Observatory, at about 0.05 ky.
7. Section B (step 7): long-term stress–strain response to the man-made cut at the bottom of the slope east of

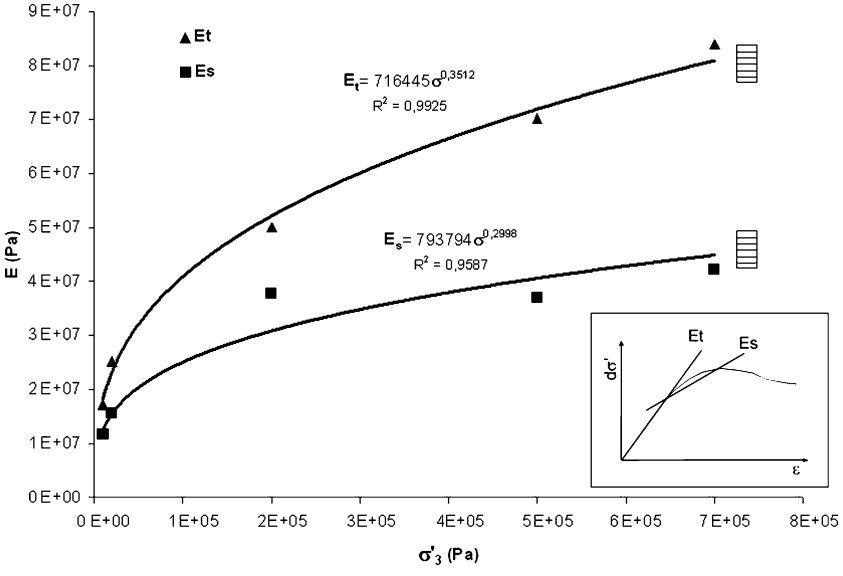

Fig. 11 Correlations between σ'_3, E_t and E_s obtained from triaxial tests on "Marne Vaticane" specimens with anisotropies oriented normally to the σ'_1

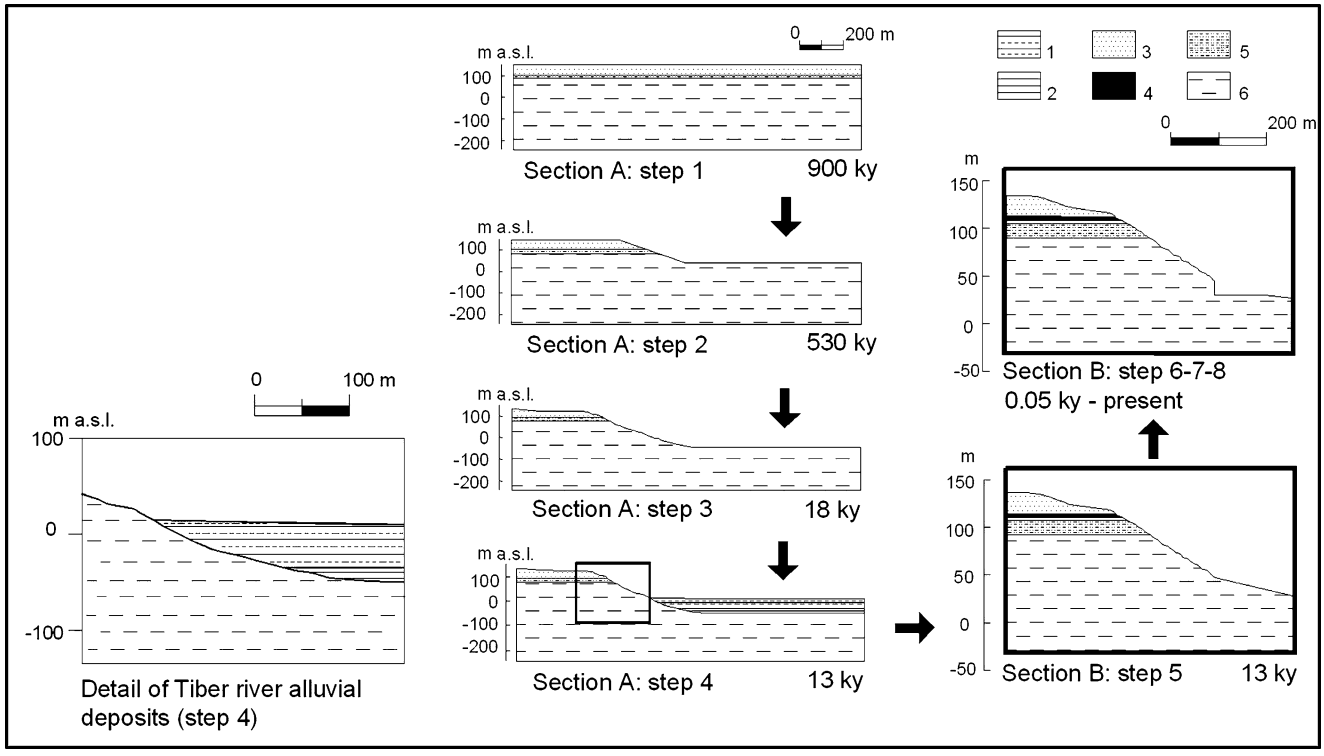

Fig. 12 Numerical model project of the slope south of the Astronomical Observatory. Reference was made to erosional and depositional events that had a significant impact on the stress–strain conditions of the rock mass (steps 1–8). *1* silty–sandy and clayey alluvial deposits of the Tiber valley; *2* coarse-grained alluvial deposits of the Tiber valley; *3* "Monte Mario" coarse-sandy grained unit; *4* "Panchina a Brachiopodi" bioclastic levels; *5* "Limi di Farneto" clayey–silty formation; *6* "Marne Vaticane" silty–clayey formation

the Astronomical Observatory, starting from about 0.05 ky.

8. Section B (step 8): time-dependent stress–strain response to the man-made cut, as a consequence of the viscous behaviour of the clayey slope east of the Astronomical Observatory, lasting about 4 years starting from about 0.05 ky.

In the above sequence, minor events (hard to define and poorly representative considering the numerical resolution of the model) were neglected.

To quantify the stress-release in the rock mass of the investigated slope, regardless of the spatial orientation of stresses, use was made of the minimum to maximum principal stress ratio ($\sigma'_{min}/\sigma'_{max}$).

The hydrogeological setting of the investigated area prior to the present time was not known. Therefore, use was made of saturated soil parameters without considering aquifers, if any. The only aquifer of the area, of small size, resides in the basal portion of the Monte

Table 3 Values of parameters used in numerical simulations

Deposits	Density (kg/m^3)	ϕ (°)	c_i (Pa)	t (Pa)	dil (°)	E_t (Pa)	E_s (Pa)	v
Marne Vaticane clayey silt	2,110	$10.62\ln(\sigma)+165.10$	$0.58\sigma+16{,}723$	1.30×10^4	14	$716{,}445\times\sigma^{0.35}$	$793{,}794\times\sigma^{0.30}$	0.25
Farneto silt	2,014	23	9.81×10^3	2.31×10^4	0	6.38×10^7	6.38×10^7	0.25
Monte Mario sand	1,850	35	0	0	0	2.37×10^8	2.37×10^8	0.25
Alluvial gravel	1,600	38	0	0	0	1.54×10^8	1.54×10^8	0.25
Alluvial clay	1,710	17	6.50×10^3	5.60×10^5	15	5.60×10^6	5.60×10^6	0.25
Alluvial silty-sand	1,750	32	1.00×10^3	8.82×10^4	0	7.00×10^6	7.00×10^6	0.25

The distribution of the "Marne Vaticane" silty-clays parameters as a function of confining pressures was used in all evolutionary steps, except in step 8 (creep configuration); in the latter case, use was made of average parameter values referred as $\sigma'_3 = 2.7e5$ Pa*den* density; φ friction angle; c_i intercept cohesion; t tension cut-off; *dil* dilation angle; E_t Young modulus; E_s elasto-plastic secant modulus; v Poisson ratio

Mario unit and is bounded, at its base, by the ''Marne Vaticane'' unit.

The contour of the $\sigma'_{min}/\sigma'_{max}$ ratio clearly shows that, with respect to initial conditions (step 1), the stress-release in the slope takes place as early as in the first erosional step (step 2), along the belt which is on average parallel to ground level and about 60 m thick (Fig. 13a). In this belt, the $\sigma'_{min}/\sigma'_{max}$ ratio is generally equal to 0.3–0.4, except in the ''Limi di Farneto'' silts, where its value is about 0.5. Outside the stress-released belt, the $\sigma'_{min}/\sigma'_{max}$ ratio corresponds to the coefficient of lateral stress at rest (K_0) and takes on a value of 0.6. This value is in line with site test measurements resulting from technical reports, in spite of the high OCR value of the investigated stiff clays.

In the second erosional step (step 3), the material whose stress has been released in the previous erosional step (step 2) is removed and the slope undergoes a new stress-release process (Fig. 13b). In this step, the volume of material undergoing stress-release is much higher than in the previous step; indeed, the value of $\sigma'_{min}/\sigma'_{max}$ reaches 0.3–0.4 for an about 70-m-thick belt. It is worth noting that the same ratio drops to 0.2 above 40 m a.s.l. for an about 30-m-thick belt.

During sedimentation of recent alluvia (step 4), the applied stress increases the $\sigma'_{min}/\sigma'_{max}$ ratio to values that are close to the ones preceding the erosional stages beneath the present alluvia of the slope (Fig. 13c).

Starting from step 5 of the simulation sequence, use was made of an engineering-geology model built along section B; additionally, the ''Marne Vaticane'' clays were assigned with strength parameters and deformation moduli which varied with confining pressures, according to laws of variation obtained from laboratory tests. For the remaining lithotypes, use was made of the strength and deformability parameters previously used in the model built along the first engineering-geology section. Given its higher resolution, the model of section B also took into consideration the presence of the ''Panchina a Brachiopodi'' level in the lower terms of the ''Sabbie Gialle di Monte Mario'' sands. Numerical simulations in groundwater configuration were not performed owing to: (1) lack of pore pressure monitoring data, (2) hydrogeological conditions of the analysed slope, where the contact between the ''Sabbie Gialle di Monte Mario'' sands and the ''Marne Vaticane'' silty clays can be regarded as a ''no flow'' limit.

Before simulating the man-made cut at the bottom of the slope, the model reached static gravitational equilibrium, using the stress conditions resulting from the previous simulation step (step 4, section A) as input data.

In the stress solution obtained in step 5, stress-release from natural processes has a roughly parallel distribution along an about 50-m-thick belt; here, the $\sigma'_{min}/\sigma'_{max}$ ratio falls below 0.4, whilst in the shallower 15 m, its value is below 0.3 (Fig. 14a).

The effect of the man-made cut was simulated in step 6, by changing the geometry of the bottom of the natural slope and by automatically assigning the values resulting from CIU triaxial tests to all the ''Marne Vaticane'' clays whose pressure unloading had exceeded the conditions prior to the man-made cut by 10% (thereby simulating undrained conditions for this portion of the rock mass).

The result shows that the man-made cut at the toe of the slope induces a preferential vertical stress-release, extending about 30 m upslope of the same cut. This process creates a highly stress-released wedge with a maximum displacement of 0.15 m. However, the rock mass does not reach failure conditions.

In the subsequent simulation step (step 7), by assigning the values obtained from CID laboratory tests to the entire ''Marne Vaticane'' rock mass, the $\sigma'_{min}/\sigma'_{max}$ ratio does not significantly change versus previous undrained conditions (Fig. 14b).

In the last simulation step (step 8), the model was configured in the creep mode. In this instance, the ''Marne Vaticane'' clays were characterised with the average deformation moduli obtained from laboratory tests; moreover, their rheological behaviour was changed by adding a visco-elastic element in series to the Mohr–Coulomb elastic-perfectly plastic element; for the visco-elastic element, a conservative G_R/G_0 (= retardation modulus/elastic shear modulus) ratio of 1 was assumed. This approach was taken in view of simulations previously made for analysing the viscous behaviour of the ''Marne Vaticane'' unit after the excavation of a tunnel in the city of Rome (Bozzano et al. 2003). The simulated time is about 4 years and corresponds to the period elapsing from the excavation (1955) to the construction of the retaining wall (1959).

In this case, metre-scale horizontal deformations in the vertical scarp give rise to tensile stresses upslope of the excavation, justifying the cracks that were observed along the slope (Fig. 15). Nevertheless, also in this case, the deformations are consistent with the strength of the material and no plasticity zones occur within the rock mass.

Furthermore, stress–strain analysis pointed out that the part of the slope in which the sands of the Monte Mario unit outcrop can be locally involved in shallow roto-translational slides; for this reason, in the high-resolution model along section B, an elastic behaviour was assigned to the Monte Mario unit, in order to carry on the stress–strain analysis downslope, where the ''Marne Vaticane'' stiff clays outcrop.

Discussion

Stress–strain analysis applied to the case study tested a sequential simulation approach. This approach made it possible to model the sequence of evolutionary stages

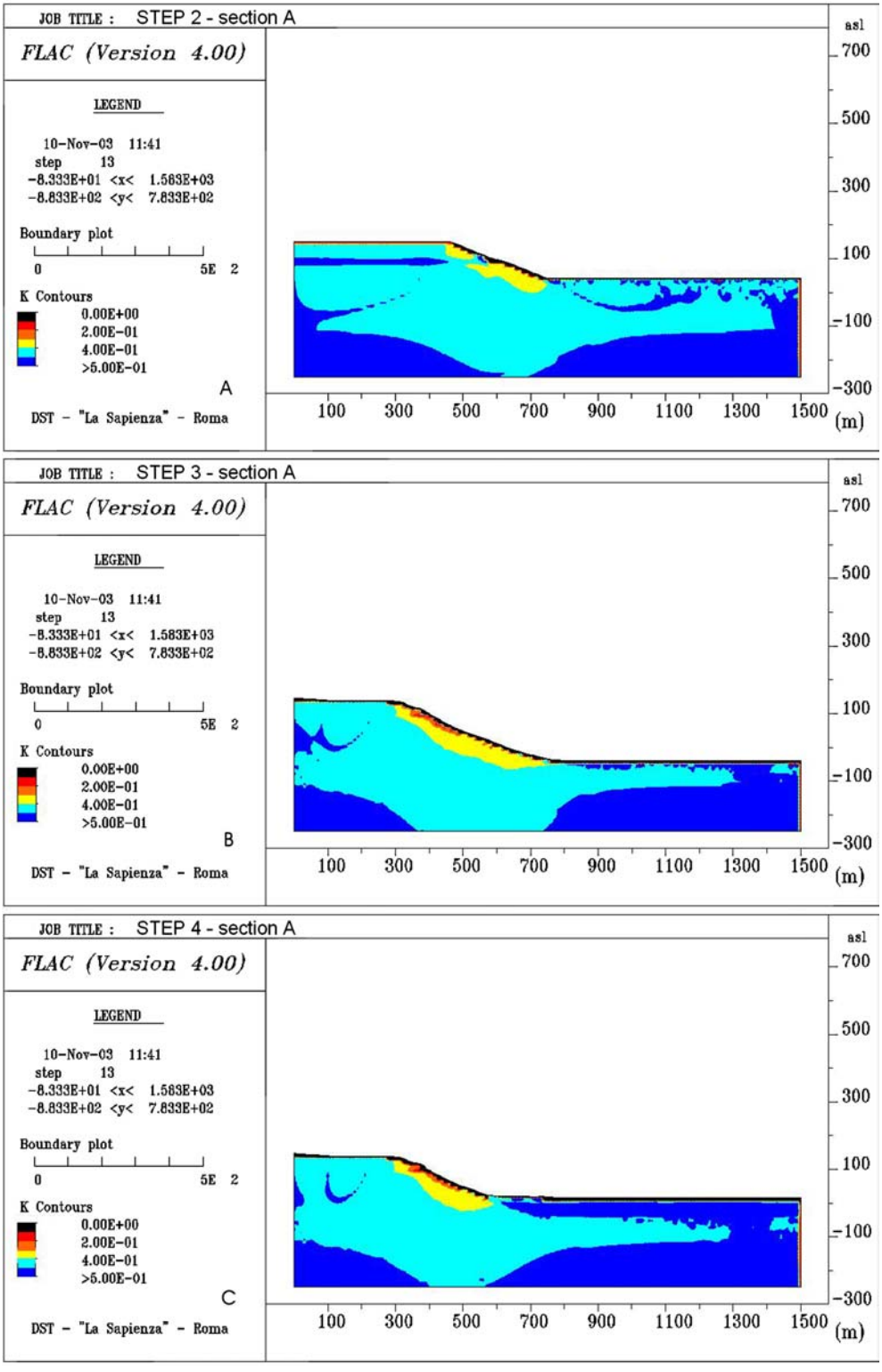

Fig. 13 Numerical simulation along section A (Fig. 12): **a** contour of $\sigma'_{min}/\sigma'_{max}$ ratio in step 2 (Tiber valley at about 530 ky); **b** contour of $\sigma'_{min}/\sigma'_{max}$ ratio in step 3 (Tiber valley at about 18 ky); **c** contour of $\sigma'_{min}/\sigma'_{max}$ ratio in step 4 (present Tiber valley)

that led to the present morphological and stratigraphic configuration of the Tiber valley in the area of the Monte Mario hill of Rome (Italy), according to the conceptual approach already proposed by Agliardi et al. (2001) and also developed by Maffei (2005) for gravity-induced slope deformations at a large spatial and temporal scale.

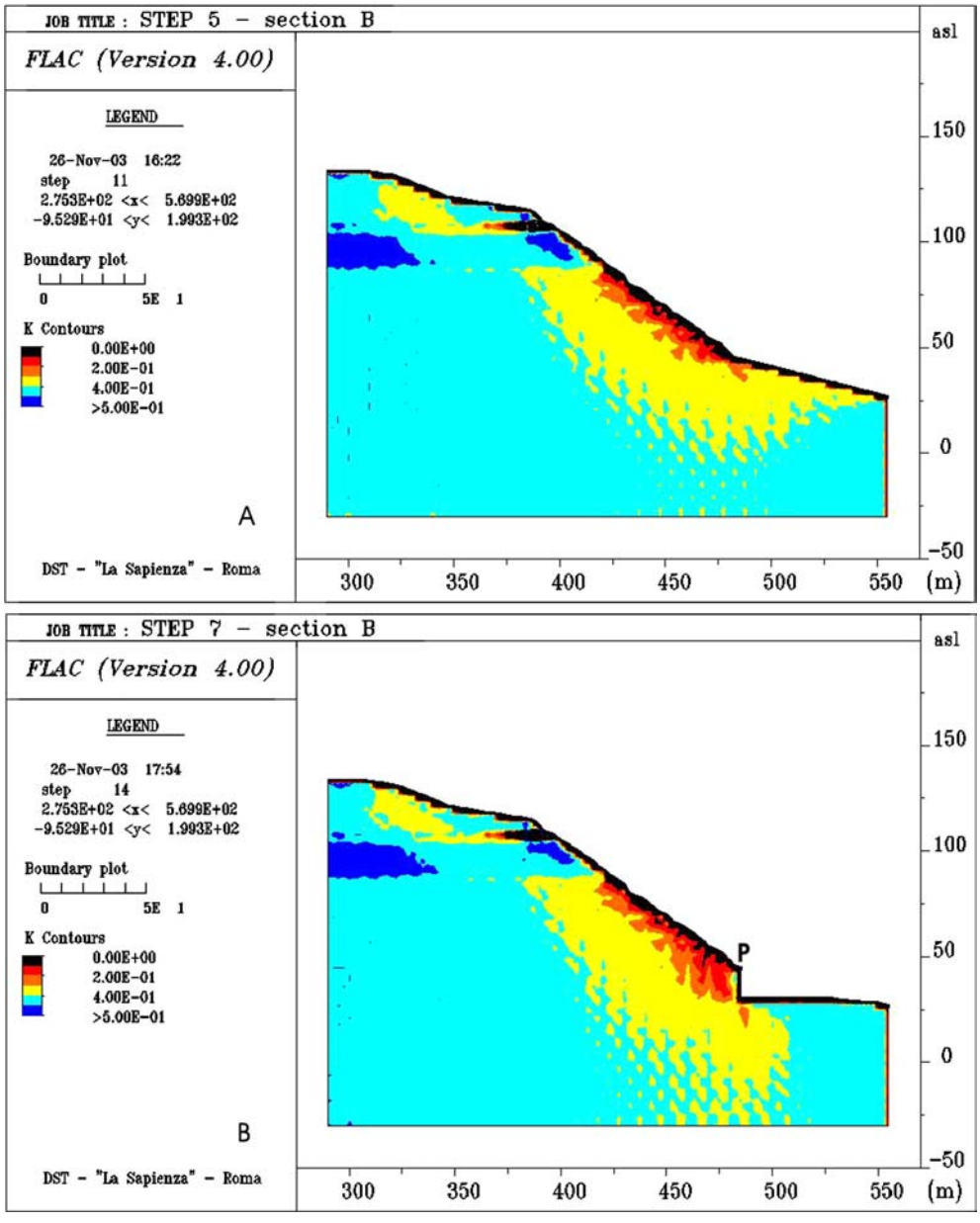

Fig. 14 Numerical simulation along section B (Fig. 12): **a** contour of $\sigma'_{min}/\sigma'_{max}$ ratio in step 5 (slope before man-made cut); **b** contour of $\sigma'_{min}/\sigma'_{max}$ ratio in step 6 (slope with man-made cut)

Numerical simulations were supported by in-site investigations and geotechnical laboratory characterisation of stiff clays ascribable to the ''Marne Vaticane'' unit. Taking into account the presumable stress history of these stiff clays, laboratory tests were aimed at defining their deformational behaviour and mechanical strength at low levels of stress as suggested by Burland et al. (1999) for stiff clay. The obtained results demonstrate the significant reduction in the mechanical shear strength of the ''Marne Vaticane'' clays and deformability moduli at the lowest tested levels of stress; in this regard, Hoque and Tatsuoka (2004) recently analysed the effects of stress on small-strain stiffness during triaxial shearing while Houlsby et al. (2005) observed a stress-dependent behaviour of elastic moduli of soils.

Stress–strain analysis, conducted via sequential modelling and supported by the Tiber valley reference engineering-geology model (sensu Fookes 1997 and Fookes et al. 2000), quantified the stress-release effects that natural processes of fluvial valley incision induced on the slope where the ''Marne Vaticane'' outcrop. These processes generated stress-release belts with a thickness of some tens of metres, circa parallel to the slope surface where the $\sigma'_{min}/\sigma'_{max}$ ratio decreases to about 0.35, starting from values at rest of about 0.6 (Fig. 16).

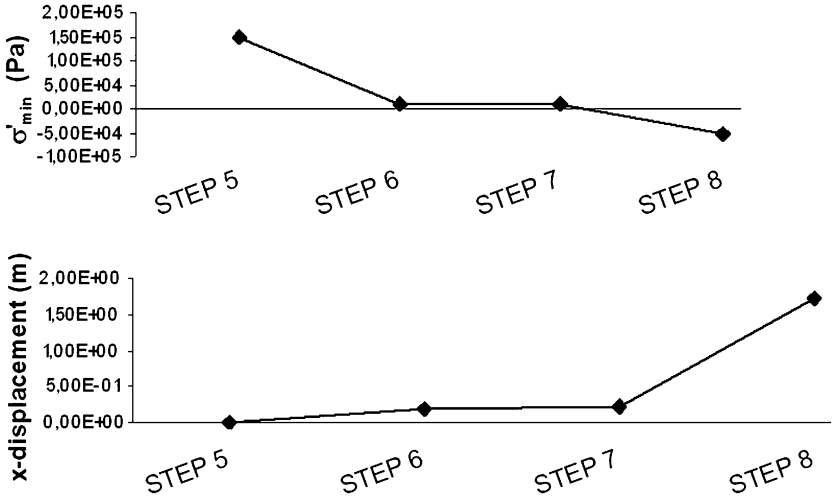

Fig. 15 σ'_{min} and horizontal displacements recorded in the steps 5–8 at point P of Fig. 14b

The tension field produced by man-made cuts is compounded by a natural stress-release wedge. The stress-release belts within this wedge (showed by the distribution of the $\sigma'_{min}/\sigma'_{max}$ ratio) become circa vertical, as they involve previously stress-released portions of the rock mass circa parallel to the slope surface. The further decrease of the $\sigma'_{min}/\sigma'_{max}$ ratio induces deformations that slightly exceed 1 m and that depend on the viscosity of the affected material. In addition, specific stratigraphic conditions (e.g. highly cemented stiff levels) control the type of landslides that are observed especially in the upper portions of the slopes.

The lack of pore pressure monitoring data does not allow to quantify the delay in the stress-release response of the slopes related to dissipation of excess pore pressures according to the findings by Potts et al. (1997). Nevertheless, stress–strain modelling of man-made cuts was sequentially performed under total stress and effective stress conditions, using parameters from laboratory triaxial tests, in order to take into account the long-term variation of the stiff clay strength.

Fig. 16 Block diagram showing the stress–strain evolution of the Monte Mario slope as a consequence of man-made cuts. *1*: *a* fill material, *b* vertical man-made cut; *2*: *a* fine-grained alluvial deposits, *b* coarse-grained slope debris and alluvial deposits; *3* "Marne Vaticane" silty-clays; *4* "Limi di Farneto" silts; *5* "Panchina a Brachiopodi" bioclastic levels; *6* "Sabbie Gialle" sands of the Monte Mario unit; *7* blocks fallen from the "Panchina a Brachiopodi" levels ; *8* landslide debris; *9* joints upslope of the man-made cut, mapped on 21st November 2002 (see Fig. 9); *10* contour of the $\sigma'_{min}/\sigma'_{max}$ ratio seen in cross-section and derived from stress–strain simulation (see Fig. 14): *a* $\sigma'_{min}/\sigma'_{max} > 0.4$, *b* $0.3 < \sigma'_{min}/\sigma'_{max} < 0.4$, *c* $0.2 < \sigma'_{min}/\sigma'_{max} < 0.3$, *d* $0.1 < \sigma'_{min}/\sigma'_{max} < 0.2$

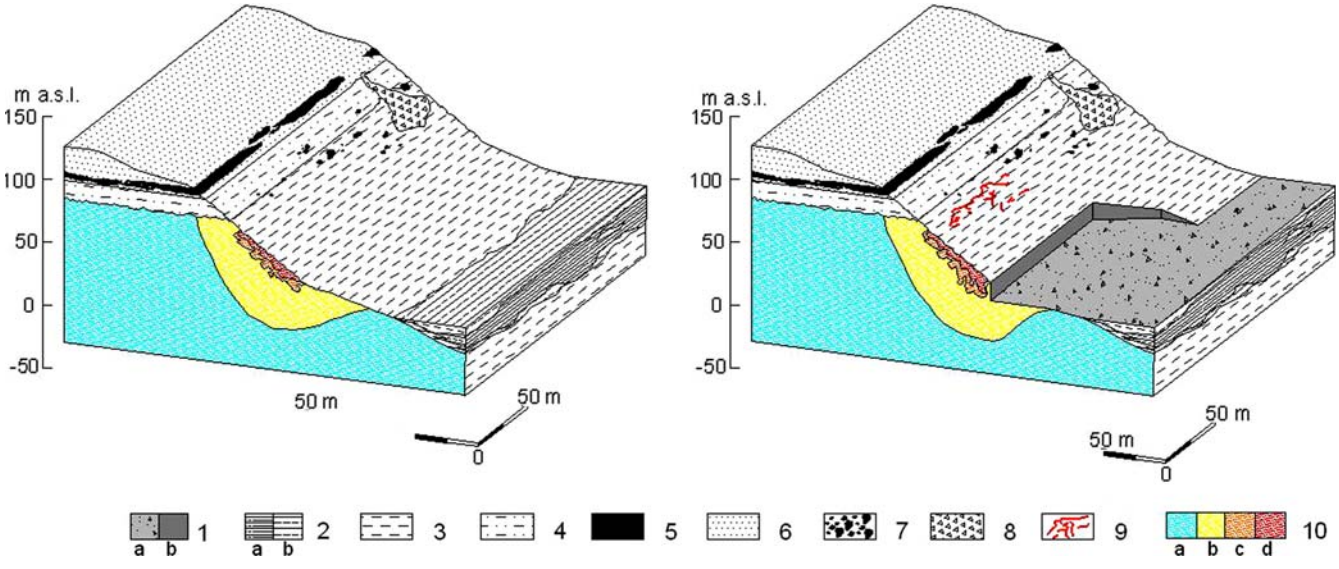

Conclusions

The case study highlights the fundamental role that both natural erosion and man-made cuts along the slope play in terms of stress release. The tensional effect of the two contributions on the stress field are distinguishable both in geometry and magnitude: more extensively stress-released zones, circa parallel to the topographic surface, are due to natural erosional processes while local concentrated stress-released subvertical belts or wedges are a consequence of downslope man-made cuts. The resulting superimposition of natural and man-induced stress-release effects can induce failure conditions within the natural stress-released portion of the slopes. The delay of the effects due to man-made cuts in clayey materials can be generally referred to a time-dependent behaviour as well as to dissipation of excess pore pressure.

Laboratory data for the investigated ''Marne Vaticane'' stiff clays demonstrate that they are particularly prone to failure as a consequence of stress release, since the measured shear strength significantly decreases at low tensional level.

On the basis of historical data, the stability conditions of the investigated slope, close to the Astronomical Observatory, can be referred to the whole area of the Monte Mario hill. Moreover, the analysed evolutionary processes appear to be representative of more general conditions, since Plio-Pleistocene stiff clays widely outcrop throughout the Italian peninsula, along important fluvial valleys as well as in urban areas. Owing to their shallow stratigraphic position, these lithotypes commonly interact with anthropic structures, as well as with quarrying activities, but are also subject to major erosional processes due to natural morphogenic actions.

Acknowledgements The author thanks F. Marra and A. Prestininzi for their scientific review of this paper and for their personal communications; the authors are also indebted to Roma Natura for providing technical documentation about the ''Parco di Monte Mario'' area and to Astaldy Company for the access to the ''Passante a NW'' tunnel during its construction. Publication of this paper was funded by grants of the Earth Science Department of the University of Rome ''La Sapienza'' (MIUR ''ex 60%'', responsible Dr. M. Gaeta).

References

Agliardi F, Crosta G, Zanchi A (2001) Structural constraints on deep-seated slope deformation kinematics. Eng Geol 59:83–102

Ambrosetti P, Bonadonna FP (1967) Revisione dei dati sul Plio-Pleistocene di Roma. Atti Accademia Gioenia di Sc Naturali In Catania 18:33–70

Amorosi A, Cotecchia F, Lollino P, Parise M, Santaloia F (2004) Instability processes of stiff clayey slopes subjected to excavation. In: Lacerda WA, Ehrlich M, Fontoyra SAB, Sayao SF (eds) Landslides: evaluation and stabilization, Proceedings of the IX international symposium on landslides (Rio de Janeiro). Balkema, Rotterdam, pp 1201–1206

Asef MR, Reddish DJ (2002) The impact of confining stress on the rock mass deformation modulus. Géotechnique 52(4):235–241

Bellotti P, Chiocchini U, Castorina F, Tolomeo L (1994) Le Unità clastiche plio-pleistoceniche tra Monte Mario (città di Roma) e la costa tirrenica presso Focene: alcune osservazioni sulla stratigrafia sequenziale. Boll. Serv. Geol. d'Italia CXIII: 3–24

Belluomini G (1985) Risultati e prospettive di un nuovo metodo di datazione basato sulla racemizzazione degli Amminoacidi. Acc. Naz. dei Lincei, Contr. Centro Interd. di Sc. Mat. e loro Appl., 69

Bergamin L, Carboni MG, Di Bella L, Marra F, Palagi I (2000) Stratigraphical and paleoenvironmental features of the Pleistocene sediments of Monte Mario (Rome). Eclogae Geologicae Helvetiae 93(2):265–275

Bonadonna FP (1968) Studi sul Pleistocene del Lazio V. La biostratigrafia di Monte Mario e la ''Fauna Malacologica Mariana'' di Cerulli Irelli. Mem Soc Geol It 7:261–321

Bozzano F, Andreucci A, Gaeta M, Salucci R (2000) A geological model of the buried Tiber River Valley beneath the historical centre of Rome. Bull Eng Geol Env 59:1–21

Bozzano F, Martino M, Martino S, Moretti S, Zannotti S (2003) Analysis of deformations in the ''argille grigio-azzurre'' formation based on site observations, vol 1. Congresso AIGA (Chieti, 18–20/02/2003) (abstract)

Burland JB, Longworth TI, Moore JFA (1977) A study of ground movement and progressive failure caused by a deep excavation in Oxford Clay. Géotechnique 27(4):557–591

Burland JB, Rampello S, Georgiannou VN, Calabresi G (1999) A laboratory study of the strength of four stiff clays. Géotechnique 49(2):273–283

Calabresi G (2004) Terreni argillosi consistenti: esperienze italiane. Rivista Italiana di Geotecnica 38(1):14–57

Cancelli A, Chinaglia N (1993) Shear strength parameters and slope stability in argillaceous rocks. In: Anagnostopoulos CA et al (eds) Geotechnical engineering of hard soil-soft rocks. Balkema, Rotterdam, pp 1087–1092

Calabresi G, Scarpelli G (1985) Argille sovraconsolidate e fessurate: fenomeni franosi. Geologia Applicata ed Idrogeologia XX(II):93–125

Calabresi G, Rampello S, Viggiani G (1990) Il comportamento meccanico delle argille consistenti. Atti MIR '90 (1990 MIR proceedings), III ciclo di conferenze di meccanica ed ingegneria delle rocce (3rd series of rock mechanics and engineering conferences) 3:1–16

Carboni MG (1975) Biostratigrafia di alcuni affioramenti pliocenici del versante tirrenico dell'Italia centrale. Geologica Romana 14:63–85

Chandler RJ, Skempton AW (1974) The design of permanent cutting slopes in stiff fissured clays. Géotechnique 24(4):457–466

Conato V, Esu D, Malatesta A, Zarlenga F (1980) New data on the Pleistocene of Rome. Quaternaria 22:131–176
Cooper MR, Broomhead EN, Petley DJ, Grants DI (1998) The Selborne cutting stability experiment, Géotechnique 48(1):63–102
Cosentino D, Cipollari P, Di Bella L, Esposito A, Faranda C, Giordano G, Gliozzi E, Mazzini I, Moretti S, Funiciello R (2004) Il limite Plio-Pleistocene nella città di Roma: nuovi dati di sottosuolo dal Passante a Nord Ovest (Monte della Farnesina). Atti del Convegno Geosed, Roma
De Angelis D'Ossat G (1942) Nuove sezioni geologiche dei colli di Roma. Boll Soc Geol It 61:22–49
Dixon N, Bromhead EN (2002) Landsliding in London Clay coastal cliffs. Q J Eng Geol Hydrogeol 35:327–343
Duncan JM, Dunlop P (1969) Slopes in stiff-fissured clays and shales. J Soil Mech Found Div ASCE 95(5):467–492
Esu F (1966) Short-term stability of slopes in unweathered jointed clays. Géotechnique 16(4):321–328
Fookes PG (1997) The First Glossop lecture. Geology for Engineers the Geological Model, Prediction and Performance. Q J Eng Geol Hydrogeol 30:293–424
Fookes PG, Baynes FJ, Hutchinson JN (2000) Invited lecture, Total geological history: a model approach to the anticipation, observation and understanding of site conditions. GeoEng 2000, an international conference on geotechnical and geological engineering, vol 1. Melbourne, pp 370–460
Frutaz AP (1962) Le piante di Roma. Istituto di Studi Romani
Gigli E (1971) Cosa c'è sotto Roma? Monte Mario, Vaticano, Gianicolo: una sola origine. Capitolium 46:7–8
Giordano G, Esposito A, De Rita D, Fabri M, Mazzini I, Trigari A, Rosa C, Funiciello R (2003) The sedimentation along the Roman Coast between Middle and Upper Pleistocene: the interplay of eustatism, tectonics and volcanism—new data and review. II Quaternario 16(1bis):121–129
Griffith AA (1920) The phenomena of rupture and flow in solids. Phil Trans Roy Soc London A 221:163–198
Griffith DV, Fenton GA (2000) Influence of soil strength spatial variability on the stability of an undrained clay slope by finite elements. Slope Stability 2000, Proceedings of the sessions of Geo-Denver 2000, ASCE, pp184–193
Haneberg WC (1999) Effect of valley incision on the subsurface state of stress-theory and application to the Rio Grande Valley near Albuquerque, New Mexico. Environ Eng Geosci V(1):117–131
Hicks MA, Samy K (2002) Influence of heterogeneity on undrained clay slope stability. Q J Eng Geol Hydrogeol 35:41–49
Hoque E, Tatsuoka F (2004) Effect of stress ratio on small-strain stiffness during triaxial shearing. Geotecnique 54(7):429–439
Houlsby GT, Amorosi A, Rojas E (2005) Elastic moduli of soils dependent on pressure: a hyperelastic formulation. Geotecnique 55(5):383–392
IGM (1924) Roma e suburbio. In Frutaz (1962): Le piante di Roma. Istituto di Studi Romani
Itasca (2000) FLAC 4.0: user manual. Itasca Consulting Group (License: DST- ''La Sapienza'', Roma, Serial number 213-039-0127-16143)
Karner DB, Marra F (1998) Correlation of fluviodeltaic aggradational sections with glacial climate history: a revision of the Pleistocene stratigraphy of Rome. Geol Soc Am Bull 110(6):748–758
Karner DB, Marra F, Renne PR (2001a) The history of the Monti Sabatini and Alban Hills volcanoes: groundwork for assessing volcanic-tectonic hazards for Rome. J Volcanol Geotherm Res 107:185–219
Karner D, Marra F, Florindo F, Boschi E (2001b) Pulsed uplift estimated from terrace elevations in the coast of Rome: evidence for a new phase of volcanic activity? Earth Planet Sci Lett 188:135–148
Leroueil S (2001) Natural slopes and cuts: movement and failure mechanisms. Géotechnique 51(3):197–243
Maffei A, Martino S, Prestininzi A (2005) From the geological to the numerical model in the analysis of gravity-induced slope deformations: an example from the Central Apennines (Italy). Eng Geol 78:215–236
Malatesta A, Zarlenga F (1986) Evoluzione paleogeografico-strutturale plio-pleistocenica del basso bacino romano a nord e a sud del. Tevere Mem Soc Geol It 35:75–85
Marino A, Gigli M (1934) Roma. In Frutaz (1962): Le piante di Roma. Istituto di Studi Romani
Marra F (1993) Stratigrafia ed assetto geologico-strutturale dell'area romana compresa tra il Tevere ed il Rio Galeria. Geologica Romana 29:515–535
Marra F, Rosa C (1995a) Stratigrafia ed assetto geologico dell'area romana. In: Funiciello R. (ed) La geologia di Roma. Il centro storico. Mem. Descr. Carta Geologica d'Italia, vol 50, pp 49–112
Marra F, Rosa C (1995b) Carta geologica del centro storico di Roma in scala 1:10000. In: Funiciello R (ed) La geologia di Roma. Il centro storico. Tav. 9. Mem. Descr. Carta Geologica d'Italia, p 50
Marra F, Rosa C, De Rita D, Funiciello R (1998) Stratigraphic and tectonic features of Middle Pleistocene sedimentary and volcanic deposit in the area of Rome (Italy). Q Int 47–48:51–63
Matheson DS, Thomson S (1973) Geological implications of valley rebound. Can Gothec J 10:961–977
McTingue DF, Mei CC (1981) Gravity-induced stresses near topography of small slope. J Geophys Res 86(B10):9268–9278
Miller DJ, Dunne T (1996) Topographic perturbations of regional stresses and consequent bedrock fracturing. J Geophys Res 101(B11):25,523–25,536
Milli S (1997) Depositional setting and high-frequency sequence stratigraphy of the Middle-Upper Pleistocene to Holocene deposits of the Roman Basin. Geologica Romana 33:99–136
Potts DM (2003) Numerical analysis: a virtual dream or practical reality? Géotechnique 53(6):535–573
Potts DM, Kovacevic N, Vaughan PR (1997) Delayed collapse of cut slopes in stiff clay. Géotechnique 47(5):953–982
Rampello S, Silvestri S (1993) The stress–strain behaviour of natural and reconstituted samples of two overconsolidated clays. In: Anagnostopoulos CA et al (eds) Geotechnical engineering of hard soils-soft rocks. Balkema, Rotterdam, pp 769–777
Savage WZ, Swolfs HS, Powers PS (1985) Gravitational stresses I longsymmetric ridges and valleys. Int J Rock Mech Min Sci Geomech Abstr 22(5):291–302
Spina G (1958) Risultati di prove eseguite sull'argilla di Monte Mario (Roma). Giornale del Genio Civile, pp 112–115
Skempton AW (1977) Slope stability of cutting in Brown London clays. Proc 9th Inter Conf Soil Mech Found Eng 3:261–270
Tavenas F, Leroueil S (1980) Creep and failure of slopes in clays. Can Gothec J 18:106–120
Vaughan PR (1994) Assumption, prediction and reality in geotechnical engineering. Géotechnique 44(4):573–609
Ventriglia U (1986) Unpublished technical report
Ventriglia U (2002) La geologia del territorio del comune di Roma. Amministrazione Provinciale di Roma, Roma, pp. 809, 13 Tav